~~The~~ ENSO~~-driven~~ ~~bias~~ contribution to~~in~~ the assessment of long-term cloud feedback to global warming

Huan Liu[1], Ilan Koren[2], Orit Altaratz[2], Shutian Mu[1]

[1]College of Meteorology and Oceanography, National University of Defense Technology, Changsha, 410073, China
[2]Department of Earth and Planetary Sciences, Weizmann Institute of Science, Rehovot, 76100, Israel

Correspondence to: Huan Liu (huanliu@nudt.edu.cn)

Abstract. Accurately assessing ~~the~~ cloud feedback to global warming is essential for producing reliable climate projections. Linear regression analysis is a widely used method for this purpose, offering a straightforward approach for examining the relationship between cloud radiative effects and ~~global~~ global-mean surface temperature. However, the El Niño–Southern Oscillation (ENSO) can ~~introduce a~~ significantly contribute to ~~bias in~~ these ~~estimations~~estimates, which is often overlooked due to ENSO's relatively short periodicity (2–7 years). Using 72 years of reanalysis data and 150 years of simulations by ~~12~~ 11 global climate models, this study demonstrates that, over large portion of the low- to mid-latitude oceans, ENSO can contribute up to a few W m^{-2} K^{-1}~~produce a bias of comparable magnitude~~ to the regression-based ~~estimated~~ cloud feedback estimates, over decades and even centuries. By providing a detailed spatial and temporal analysis~~ of this bias~~, our findings underscore the importance of accounting for and removing ~~the~~ ENSO's influence to improve the accuracy of cloud feedback assessments in the context of global warming.

1 Introduction

Clouds, which cover over 50% of the Earth's surface, play a critical role in regulating the Earth's energy budget (Stubenrauch et al., 2013). They reflect incoming solar radiation (~~S~~short~~ W~~wave ~~C~~cloud r~~R~~adiative ~~E~~effect, CRE_{SW}) and trap outgoing terrestrial radiation (~~L~~long~~ W~~wave ~~C~~cloud ~~R~~radiative ~~E~~effect, CRE_{LW}), resulting in a net cooling effect (net cloud radiative effect, CRE_{net}) of approximately 20 W m^{-2} at the top~~-~~ of~~- the~~ atmosphere (~~net Cloud Radiative Effect, CRE_{net}~~TOA) (Stephens et al., 2012). This fundamental role makes cloud response to global warming (cloud feedback) a key factor in climate change ~~predictions~~ projections (Zelinka et al., 2020). However, both the magnitude and sign ~~(positive for additional warming, negative for cooling)~~ of cloud feedback (positive for amplifying warming, negative for damping warming) remain uncertain in the assessments of current global climate models (GCMs), ~~contributing~~ dominating the spread ~~to significant discrepancies~~ in estimates of equilibrium climate sensitivity (Forster et al., 2021).

One major source of the uncertainty in estimates of cloud feedback to global warming is the natural climate variability , caused by phenomena like the Atlantic Multi-decadal Variability, the Pacific Decadal Oscillation, and the El Niño-Southern Oscillation (ENSO) (Li et al., 2021), all of which can introduce distinct ~~different~~ spatial and temporal influences ~~bias~~ across different regions and periods (Forster et al., 2021). ~~The~~ ENSO is characterized by anomalous sea-~~-~~surface temperature and sea-level pressure in the tropical Pacific, acting~~-~~ on relatively short timescales with a typical periodicity of 2–7 years~~and dominating seasonal to interannual timescales~~ (Neelin et al., 1998). By modulating ~~the~~ atmospheric dynamics and thermodynamics (Davey et al., 2014; Taschetto et al., 2020), ENSO ~~can~~ affects cloud properties (Park and Leovy, 2004; Eleftheratos et al., 2011; Teng et al., 2014; Madenach et al., 2019; Liu et al., 2023) and ~~cloud radiative effect~~CREs (Chen et al., 2000; Yang et al., 2016). Previous studies have identified an ENSO signature, on a global scale, in both the long-term warming trend (e.g., Penland and Matrosova, 2006; Compo and Sardeshmukh, 2010) and cloud feedback estimates (referred to as ENSO contribution~~-related bias~~, hereafter) (e.g., Zhou et al., 2015; Richardson et al., 2022; Uribe et al., 2022; Jin et al., 2024). For example, Richardson et al. (2022) proposed that ~~the~~ ENSO contribution~~-related bias~~ may affect estimated linear trends over short time windows of up to about 10 years. Jin et al. (2024) found that the seasonally asymmetric patterns of cloud feedback are ~~controlled~~ primarily controlled by ENSO. Nevertheless, the full influence of ENSO on cloud feedback in the context of global warming remains unclear~~is still unknown~~ and has often been overlooked due to ~~the~~ ENSO's relatively short periodicity~~ (i.e., 2–7 years)~~ (Hope et al., 2017)~~, which masks its long-term effect on cloud feedback estimates~~.

~~For~~ To partially address~~ing~~ this knowledge gap, we apply a regression-based ~~de-ENSO~~ method to correct ENSO's influence (referred to as the ENSO-correction method, hereafter), thereby quantifying the spatial distribution and timescales of ~~the~~ ENSO contribution to~~-related bias in~~ cloud feedback estimates under global warming. The remainder of this paper is organized as follows: Section 2 describes the datasets and ~~methodologies~~ methodology~~used in the analysis~~, Section 3 ~~discusses~~ presents the key findings, and Section 4 summarizes the main conclusions.

2 Materials and methods

2.1 Datasets

The primary analysis~~This study~~ uses 72 years of reanalysis data from the ERA5 dataset, 20 years of satellite measurements from the CERES EBAF product, and ~~long-term (~~150 years~~)~~ of GCM simulations from the abrupt-4×CO_2 experiment. For supplementary analysis, a 65-year segment of GCM simulations from the historical experiment is also used. The analysed variables include sea-surface temperature, air temperature at 2 meters, all-sky and clear-sky TOA shortwave flux, as well as all-sky and clear-sky TOA longwave flux. The details of the different datasets:~~by 12 Global Climate Models (GCM). Based on which, the Oceanic Niño Index (ONI) is derived for measuring ENSO activity as it is NOAA's primary indicator for monitoring ENSO's oceanic signal and is widely used in ENSO-related studies (Glantz and Ramirez, 2020). A period of large positive or negative ONI values indicates an intense warm or cold phase of ENSO (i.e., the El Niño or La Niña event, characterized by an unusual warming or cooling of the central and eastern tropical Pacific Ocean surface waters) (Neelin et al., 1998).~~

~~The datasets we use:~~ (1) ERA5 data (January 1950–December 2021). ~~The primary analysis uses m~~Monthly ERA5 data (Hershach et al., 2023) is used to analyze ENSO contribution to historical cloud feedback estimates. To facilitate a walkthrough of the method and results (a sample analysis), a representative 40-year subset (January 1982–December 2021) is used. ERA5 is~~,~~ a well~~-~~-validated and widely used dataset for studying climate trends, produced by the European Centre for Medium-Range Weather Forecasts (ECMWF) (Hersbach et al., 2020; Gulev et al., 2021). ERA5 data ~~has shown~~ shows strong agreement with observed cloud properties across both weather and climate scales and has been found to effectively capture the spatiotemporal characteristics of measured ENSO-driven changes in cloud cover (Liu et al., 2023; Yao et al., 2020; Binder et al., 2020). ~~The analyzed variables include sea surface temperature, air temperature at 2 meters, Top net Solar Radiation (TSR; the incoming minus the outgoing solar radiation at the top of the atmosphere), Top net Solar Radiation-Clear sky (TSRC; similar to RST but assuming clear sky conditions), Top net Thermal Radiation (TTR; similar to TSR but for thermal radiation), and Top net Thermal Radiation-Clear sky (TTRC; similar to TSRC but for thermal radiation). The original ERA5 resolution (0.25°) was averaged to 2° to reduce computational demands.~~

(2) CERES measurements (January 2002–December 2021). We conduct a comparison between ENSO contribution derived from ERA5 data and satellite measurements using TOA fluxes from the Earth's Radiant Energy System (CERES) Energy Balanced and Filled (EBAF) data product (Loeb et al., 2018; updated to Edition 4.2). It is specifically designed for climate trend analysis, as it minimizes errors from instrument calibration and orbital drift by integrating measurements from multiple satellites (Loeb et al., 2018). Here, this product is regarded as a benchmark observational dataset for evaluating the reanalysis of the Earth's energy budget.

(3) GCM simulations (January 1950–December 2014 for the historical experiment, and the first 150 years for the abrupt-4×CO_2 experiment~~s~~). This study uses~~Long-term~~ simulations from the historical and abrupt-4×CO_2 experiments conducted by 11~~2~~ GCMs ~~that~~ participating~~ed~~ in the Cloud Feedback Model Intercomparison Project (CFMIP) of the sixth phase of the Coupled Model Intercomparison Project (~~CFMIP-3/~~CMIP6) (Webb et al., 2017). We focus on~~All~~ the ~~selected GCM simulations use~~the variant label "r1i1p1f1"~~, which refers to a specific experiment configuration within the CMIP6 model run: the first realization with the first set of initial conditions, physics parameterizations, and external forcing conditions. As shown in Table 1, the analyzed simulations include the outputs of the historical and the abrupt-4×CO₂ experiments~~ (Eyring et al., 2016). The historical experiment spans from 1850 to 2014 and is designed to provide insights into how the observed natural and anthropogenic factors have shaped current climate conditions. In this study, the period of January ~~01.~~1950–December ~~12.~~2014 is analyzed ~~for~~ to ~~generalizing~~ generalize the results obtained by ~~the~~ ERA5 data. The abrupt-4×CO_2 experiment is a Diagnostic, Evaluation and Characterization of Klima (DECK)~~baseline~~ experiment ~~of the Diagnostic, Evaluation and Characterization of Klima (DECK) experiments that offers~~with a mandated minimum simulation period of 150 years. It is designed to evaluate the ~~immediate~~ climate response to an instantaneous ~~sudden~~ quadrupling of the prescribed pre-industrial atmospheric CO_2 concentration and ~~hence~~ is therefore widely used for assessing cloud feedback in the context of global warming. We use t~~T~~he first 150 years ~~in the~~of these simulations ~~are used~~ to investigate ~~the~~ ENSO contribution to ~~related bias in~~ cloud feedback projections~~estimates. Similar to ERA5 data, the analyzed variables include tas (air temperature at 2 meters), rsut (like TSR), rsutcs (like TSRC), rlut (like TTR), and rlutcs (like TTRC). All GCM simulations are also resampled to a spatial resolution of 2°~~.

Table 1: Information of ~~the 12~~ GCM simulations used in this study.

GCM	Center	Country	Data Version		Data DOI
			Historical	Abrupt-4×CO_2	
E3SM-1-0	UCSB, E3SM-Project, UCI	USA	v20190913	v20190718	10.22033/ESGF/CMIP6.2294
CESM2	NCAR	USA	v20190308	v20190927	10.22033/ESGF/CMIP6.2185
BCC-CSM2-MR	BCC	China	v20181126	v20181016	10.22033/ESGF/CMIP6.1725
CanESM5	CCCma	Canada	v20190429	v20190429	10.22033/ESGF/CMIP6.1303
MRI-ESM2-0	MRI	Japan	v20190222	v20190308	10.22033/ESGF/CMIP6.621
IPSL-CM6A-LR	IPSL	France	v20180803	v20190118	10.22033/ESGF/CMIP6.1534
~~TaiESM1~~	~~AS-RCEC~~	~~China~~	~~v20200623~~	~~v20200310~~	~~10.22033/ESGF/CMIP6.9684~~
GFDL-CM4	NOAA-GFDL	USA	v20180701	v20180701	10.22033/ESGF/CMIP6.1402
GISS-E2-2-~~H~~G	NASA-GISS	USA	v20191120	~~v20200115~~v20191120	10.22033/ESGF/CMIP6.~~15861~~2081
GISS-E2-1-H	NASA-GISS	USA	v20190403	v20190403	10.22033/ESGF/CMIP6.1421
MIROC6	MIROC	Japan	v20181212	v20190705	10.22033/ESGF/CMIP6.881
NorESM2-LM	NCC	Norway	v20190815	v20210118	10.22033/ESGF/CMIP6.502

2.2 Data processing

All datasets are resampled and gridded to a common spatial resolution of 2°×2° to reduce computational demands. We first derive the oceanic Niño index (ONI) from these data as the 3-month running mean of sea-surface temperature anomalies over the Niño 3.4 region (5° S–5° N, 170° W–120° W) to quantify ENSO activity. ONI is the primary indicator of National Oceanic and Atmospheric Administration (NOAA) for monitoring the oceanic component of ENSO and is widely used in related studies (Glantz and Ramirez, 2020). Periods of large positive or negative ONI values indicate intense warm or cold phases of ENSO (i.e., the El Niño or La Niña events), which are characterized by unusual warming or cooling of the central and eastern tropical Pacific Ocean surface waters, respectively (Neelin et al., 1998). Then, for each data set, our~~Taking ERA5 as an example (a similar analysis is done for the GCMs data), the~~ analysis is based on the followinga two-step approach:

(1) Calculation of monthly means. Monthly mean values of ~~cloud radiative effect~~CREs are derived as follows: CRE_{SW} is calculated as the difference between all-sky and clear-sky TOA shortwave flux~~TSR and TSRC~~; CRE_{LW} is calculated as the difference between all-sky and clear-sky TOA longwave flux~~TTR and TTRC~~; and CRE_{net} is obtained by summing CRE_{SW} and CRE_{LW}. The monthly ~~G~~global ~~M~~mean ~~S~~surface ~~T~~temperature (GMST) is calculated as the area-weighted mean of air temperature at 2 meters over the globe. ~~The Oceanic Niño Index (ONI) is calculated as the area-weighted, 3-month running mean of sea surface temperature anomalies over the Niño 3.4 region (5° S–5° N, 170° W–120° W).~~

(2) Calculation of monthly ~~deseasonalized~~ anomalies. Monthly ~~A~~anomalies of CRE_{SW}, CRE_{LW}, CRE_{net}, and GMST are calculated as deviations of each variable from its ~~monthly~~ mean annual cycle and hence are deseasonalized. This is done by subtracting, for each calendaric month, the long-term mean (calculated over the entire study period) from the corresponding monthly value~~, over the entire 72-year period. In the analysis of the GCM simulations data, the ONI is calculated with air temperature at 2 meters~~.

The area-weighted means~~spatial averages~~ are calculated by taking into account ~~consideration~~ the area of the grid cells to reduce the disproportionate influence of smaller grids near the poles~~account for a decreased contribution of smaller grids~~. The area of each grid ~~box~~ cell is estimated as the product of arc length at the corresponding latitude and longitude, considering the Earth as an oblate spheroid with a radius of 6,378.137 km at the equator and 6,356.752 km at the poles. The statistical significance of temporal trends (trends over time) and partial regression coefficients is assessed using the Hamed and Rao modified Mann-Kendall trend test (Hamed and Rao, 1998; Hussain and Mahmud, 2019) and ~~the~~ Student's t-test, respectively. The modified Mann-Kendall test is a non-parametric method that robustly handles ~~accounts for~~ serial autocorrelation.

2.3 The ~~de~~ENSO-correction method

An ~~de~~ENSO-correction method ~~procedure~~ is applied ~~used~~ to isolate and remove ~~the~~ ENSO signal from ~~cloud radiative effects~~CRE and GMST records. Various approaches~~Several methods~~ have been developed for this purpose, including those based on numerical simulations and statistical techniques ~~tools~~ such as frequency bandpass filtering~~filter~~, regression, and signal decomposition (Penland and Matrosova, 2006; Compo and Sardeshmukh, 2010; Kelly and Jones, 1996; Angell, 2000; Guan and Nigam, 2008). ~~Each method has its strengths and limitations (Compo and Sardeshmukh, 2010).~~

In this study, we use a regression-based ~~de~~ENSO-correction method ~~approach~~ due to its conceptual simplicity and computational efficiency. Specifically, we first use a bandpass filter to remove ONI variances outside the typical ~~variations beyond~~ ENSO~~'s typical~~ periodicities ~~(i.e.,~~band of 2–7 years~~;~~ (Fig. 1). This filtering isolates the core ENSO signal and helps to decouple it from other climate perturbations, like long-term trends, the Atlantic Multi-decadal Variability, and the ~~for decoupling signatures of other climate phenomena (e.g., aerosol emission, land use,~~ Pacific Decadal Oscillation. ~~and so on) on ONI.~~ Then we use an ~~O~~ordinary ~~L~~least ~~S~~squares (OLS) regression to build statistical relationship between a dependent variable (Y; e.g., CRE_{SW}, CRE_{LW}, CRE_{net} and GMST) and the independent variables of time and the bandpass-filtered ONI, with no time lag applied~~delay~~. This ~~results~~ yields~~in~~ a multivariate regression model formulated by Eq. (1):

~~(i.e.,~~ $$\hat{Y} = a \times time + b \times ONI_{filtered} + c$$ ~~;~~ (~~Eq.~~1)~~,)~~

which ~~that~~ minimizes the sum of squared residuals (Virtanen et al., 2020). Therefore, the residual calculated from this model (referred to as ~~de~~ENSO-corrected), as formulated by Eq. (2):

~~i.e.,~~ $$Y_{ENSO-\cancel{deENSO}corrected} = Y - b \times ONI_{filtered}$$ ~~;~~ (~~Eq.~~2),

removes the linear ENSO signature while preserving the underlying temporal trend in Y as effectively ~~much~~ as possible. Importantly, because Eq. (1) uses the bandpass-filtered ONI and assumes no time lag, this OLS~~-regression~~-based ~~de~~ENSO-correction method may ~~procedure~~ retains some ENSO-related variations in *Y*. These include potential low-frequency natural trends in ENSO itself and any delayed or non-linear impacts of ENSO on GMST and CREs. Consequently, this method is likely to provide a~~both non-linear and delayed components of ENSO-related variations, as well as the ENSO-induced long-~~

~~term (outside 7 years) trend effect on Y, leading to~~ conservative estimat~~ione~~e of ENSO contribution (see Section 2.4)~~s~~ (Kelly and Jones, 1996; Compo and Sardeshmukh, 2010).

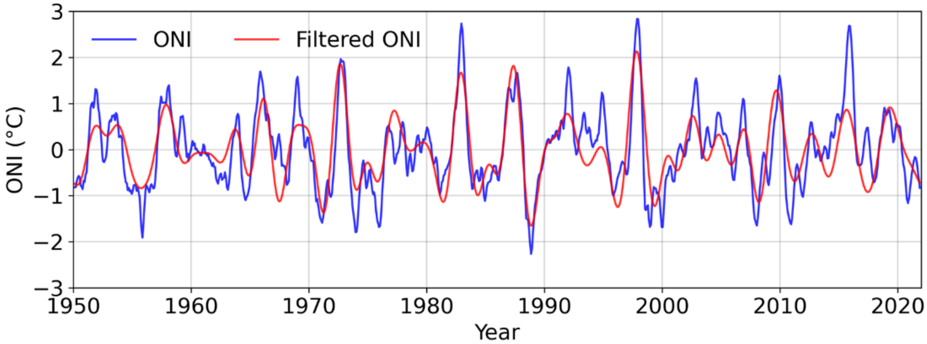

Figure 1: Time series of the original ONI (blue curve) and the bandpass-filtered ONI (red curve), derived from ~~using~~ ERA5 data during January ~~the period 01.~~1950–December ~~12.~~2021.

2.4 The estimation of ENSO contribution ~~-related bias~~

To quantify the cloud feedback to global warming, following previous studies (e.g., Clement et al., 2009; Zhou et al., 2015; Uribe et al., 2022; Ceppi and Nowack et al., 2021; Dessler, 2010), we use a common method that calculates the OLS ~~correlation~~ regression slope between ~~cloud-related properties~~CRE and ~~surface temperature~~GMST (e.g., $\frac{\partial \cancel{CRE} CRE_{net}}{\partial GMST}$). Such a method inherently captures the influence of factors affecting both global temperature and cloud properties, such as ENSO. To assess the corresponding ENSO contribution ~~-related bias~~, we compute the difference between the results obtained before and after applying the ~~de~~ENSO-correction method ~~procedure~~. This difference, as formulated in Eq. (3):

$$ENSO_{con.} = \frac{\partial CRE}{\partial GMST} - \frac{\partial CRE_{corrected}}{\partial GMST_{corrected}} \qquad (3),$$

~~-~~is then used as a proxy measure of ~~the~~ ENSO contribution to ~~-related bias in~~ cloud feedback estimates under global warming ~~(i.e., $bias = \frac{\partial CRE}{\partial GMST} - \frac{\partial CRE_{deENSO}}{\partial GMST_{deENSO}}$; Eq.3)~~.

3 Results

3.1 ENSO's impact on the global~~-~~-mean surface temperature

Figure 2 illustrates ~~examines~~ the impact of ENSO on GMST using ERA5 data from January 1950 to December 2021.

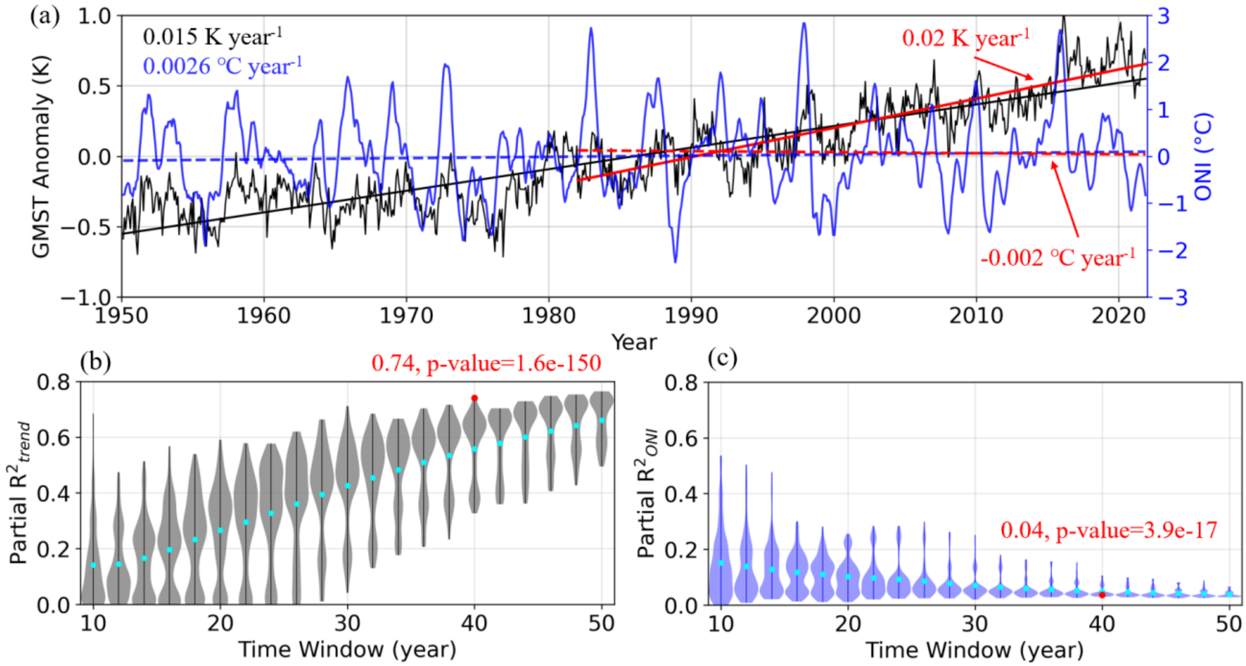

Figure 2: Analysis of the GMST variations driven by the temporal ~~warming~~ trend and ENSO, derived from ERA5 data during January ~~the period 01.~~1950–December ~~12.~~2021. (a) Time series of GMST anomaly (black curve; left y-axis) and ONI (blue curve; right y-axis). The black and blue line and number present the corresponding OLS regression line and slope, respectively. (b–c) Violin plots of (b) partial R^2_{trend} and (c) partial R^2_{ONI} for GMST, shown as a function of the time window (in intervals of 2 years). Per time window, the vertical line indicates ~~marks~~ the range (minimal to maximal), the shaded area represents the probability density, and the cyan dot denotes ~~marks~~ the mean value. ~~In this figure, t~~The red lines, dots and numbers highlight the results for the ~~randomly~~ selected representative 40-year subset ~~period~~ (January ~~1.~~1982–December ~~12.~~2021) that is analyzed in Figs. 3–~~2 and Fig.~~ 4~~a–f~~. In panel (a), s~~S~~olid and dashed lines ~~in panel (a)~~ represent the statistically significant and insignificant trends at ~~a~~ the 95% confidence level, respectively.

Figure 2a presents the time series of GMST anomalies (black curve) and the original ONI (blue curve). The corresponding OLS regression analysis reveals a consistent increase in GMST of 0.015 K year^{-1} (black line), which translates to an approximate 1 K of warming over the study period. This warming has been primarily attributed to rising CO_2 levels resulting from human activities (Eyring et al., 2021). In contrast, the ONI does not exhibit a statistically significant trend (blue dashed line), indicating no consistent long-term intensification ~~strengthening~~ or weakening of ENSO~~'s intensity in~~ over recent decades. This finding aligns with ~~3~~ 2 out of the ~~12~~ 11 GCMs (GISS-E2-2-H~~, TaiESM1~~ and E3SM-1-0), which also show no significant ENSO trend in their ~~corresponding~~ historical simulation ~~experiment~~ from 1950 to 2014 (not shown), indicating a widespread deficiency of current models in representing this historical feature of ENSO. D~~. However, d~~espite the lack of a long-term trend in ENSO, there is a clear covariation between GMST and ONI on ~~seasonal to~~ interannual timescales, highlighting ENSO's significant impact on GMST. For example, the GMST difference between the La Niña year of 1989 and the El Niño year of 1998 is approximately 0.8 K, a magnitude which is similar to the total linear warming over the entire 72-year ~~study~~ period.

~~Of course, t~~The relative contributions of the warming trend and ENSO to the variance of GMST depend on the analyzed timescale. To quantify this, we calculate the coefficient of partial determination (partial R^2) using OLS multivariate regression models (similar to Eq. (1), but using the original ONI rather than the bandpass-filtered one) and present the results as a function of the time window (ranging ~~between~~ from 10 to 50 years, ~~with a 2-year interval,~~ the upper limit of 50 years was selected to ensure an adequate ~~sufficient~~ sampl~~ing~~e size for robust analysis~~number~~). The corresponding test statistics (Fig. S1) suggest that the ONI regression coefficient (b in Eq. 1) is statistically significant at the 95% confidence level across nearly all analyses, even when the explained variance is moderate. This allows us to assess the relative contribution~~influence~~ of the warming trend ~~on GMST while controlling ONI~~ (partial R^2_{trend}~~,~~ ; Fig. 2b) and ~~the influence of ONI on GMST while controlling the warming trend~~ENSO (partial R^2_{ONI}~~,~~ ; Fig. 2c) to the total variance of GMST across different timescales with high confidence. ~~As shown, t~~The partial R^2_{trend} values increase consistently with longer time windows, suggesting that the warming trend accounts for ~~explains~~ a steadily growing proportion of GMST variance over extended periods. In contrast, the partial R^2_{ONI} values decrease yet gradually stabilize for periods exceeding ~40 years, indicating a diminishing, though progressively attenuated, influence of ENSO~~that the impact of ENSO diminishes~~ as the timescale lengthens. This inverse relationship implies that ENSO contribution to~~-related bias in~~ cloud feedback estimates becomes less substantial in~~decreases for~~ longer periods. For instance, in the~~Taking a randomly selected~~ 40-year subset from January ~~period (01.~~1982–December ~~12.~~2021~~;~~ (red dots in Fig. 2b–c)~~as an example~~, ~~while~~ the warming trend explains approximately 74% of GMST variance, whereas ~~the~~ ENSO accounts for ~~explains~~ only about 4%. The co-occurrence of this strong warming trend and the relatively weak ENSO signature, along with the stabilization of R^2_{ONI} beyond 40 years, makes this period particularly informative for examining ENSO contribution to cloud feedback estimates. It is therefore selected as a representative example to illustrate the methodology and resulting spatial patterns in Figs. 3–4. In addition, to account for the potential limitations of ONI in fully representing ENSO (Johnson, 2013), ~~Please note that~~ we conducted a similar analysis using six other ENSO indices ~~indexes to account for the potential limitations of ONI in fully representing ENSO (Johnson, 2013)~~ and got similar results (not shown).

3.2 ENSO's impact on cloud radiative effects

~~The r~~Results ~~presented~~ in Fig. 2 demonstrate the known difference in time scales between the interannual variability~~short periodicity~~ of ENSO and the persistent long-term ~~longer~~ warming trend~~,~~ over recent decades. This known difference led in the past to the neglect of ~~the~~ ENSO contribution~~-related~~ ~~bias~~ when estimating cloud feedback over long periods. However, such neglect~~This assumption~~ does not take into account the stronger impact of ENSO on clouds' properties compared to the impact of ~~the~~ recent warming ~~effect~~ (Li et al., 2021; Liu et al., 2023). To illustrate ~~further investigate~~ this point, we analyze the same 40-year period (January ~~01.~~1982–December ~~12.~~2021) as an example and present the corresponding partial R^2 maps of CREs in Fig. 3. The maps of corresponding residual R^2 are shown in Fig. S2.~~between cloud radiative effects and the ENSO, and warming signals (Fig. 3) as an example.~~

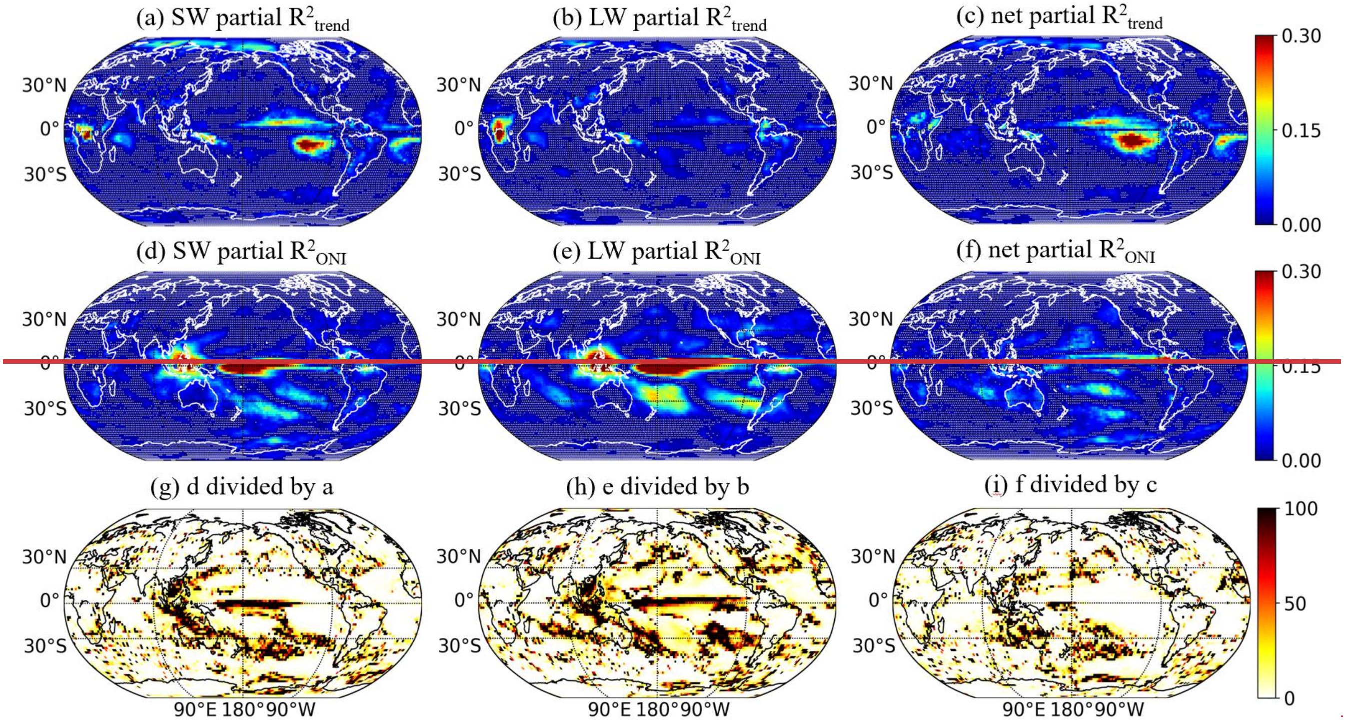

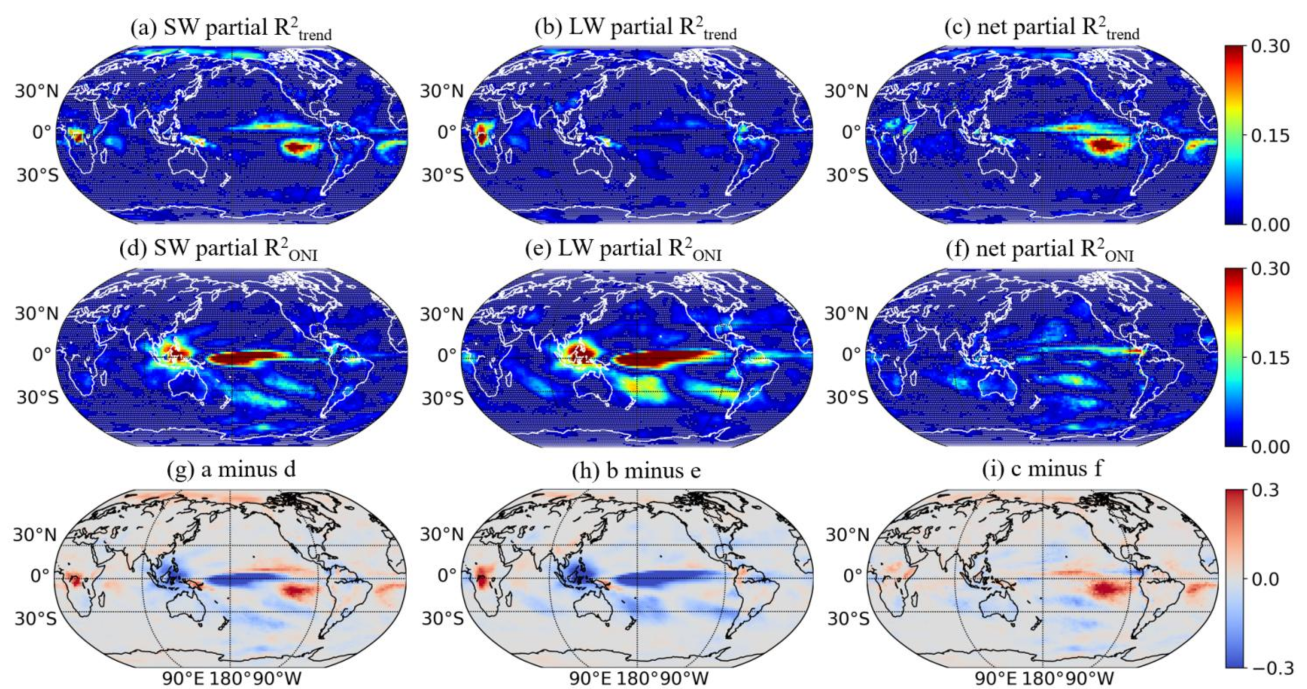

Figure 3: A sample analysis of ~~the~~ variations in ~~cloud radiative effect~~CREs as driven by the temporal ~~warming~~ trend and ENSO, derived from ERA5 data during January ~~taking the period of 01.~~1982–December ~~12.~~2021 ~~as an example~~. (a–c) ~~Variations driven by the warming trend (p~~Partial R^2_{trend}~~)~~ for ~~in~~ (a) CRE_{SW}, (b) CRE_{LW}, and (c) CRE_{net}. (d–f) ~~Variations driven by ENSO (p~~Partial R^2_{ONI}~~)~~ for ~~in~~ (d) CRE_{SW}, (e) CRE_{LW}, and (f) CRE_{net}. (g–i) The difference ~~ratio~~ between (~~d~~a–~~f~~c) and (~~a~~d–~~e~~f). In panels (a–f), white dots

denote grids with statistically insignificant partial regression coefficients of time (i.e., a in Eq. 1) and ONI (i.e., b in Eq. 1) at the 95% confidence level.

Figure 3a–c shows ~~presents~~ the spatial distribution of variations in CRE_{SW}, CRE_{LW}, and CRE_{net} attributed to the temporal ~~warming~~ trend ~~while controlling ONI~~ (partial R^2_{trend}). Given the significant warming trend in GMST during this period (0.02 K year^{-1}), t~~T~~he resulting patterns reveal ~~highlight~~ strong co-variations between CREs ~~clouds~~ and recent ~~the~~ warming ~~trend~~ in regions such as the Arctic, central ~~Middle~~ Africa, and the tropical eastern oceans. Figure 3d–f illustrates the variations in CREs attributed to~~cloud radiative effects driven by~~ ENSO ~~while controlling the warming trend~~ (partial R^2_{ONI}), with patterns agrees well with previous findings revealing the influence of ENSO in cloud properties (Yang et al., 2016; Li et al., 2021; Liu et al., 2023). Figure 3g–i displays the difference ~~ratio~~ between the two, the partial ~~R^2_{ONI}–~~R^2_{trend} minus the partial ~~and R^2_{trend}–~~R^2_{ONI}~~.~~ ~~(Fig. 2d–f divided by Fig. 2a–c). It's clear that, c~~Compared to ENSO, the ~~warming~~ temporal trend~~, although the ENSO~~ has a much weaker ~~smaller~~ impact on CREs~~the GMST during this period, the ENSO's impact on cloud radiative effects~~ over a large portion of low- to middle-latitude oceans~~-~~ (bluish shades in Fig. 3g–i)~~is significantly stronger~~. ~~And t~~This is particularly evident for CRE_{SW} and CRE_{LW} across the Pacific, ~~where the ratio reaches values around 100 (blackish shades in Fig. 3g–i),~~ implying a region-dependent ENSO contribution to ~~related bias in~~ the assessment ~~estimation~~ of long-term cloud feedback to global warming.

3.3 ENSO contribution to ~~related bias in estimating~~ historical cloud feedback estimates~~to global warming~~

Next, we examine ~~the~~ ENSO contribution (see Section 2.4) to historical~~related bias in~~ cloud feedback estimates. To illustrate the methodology~~Following the deENSO method (Section 2.3)~~, Fig. 4 shows results~~a–f presents the ENSO-related bias calculated~~ for the same ~~exampled~~ 40-year period (January ~~01.~~1982–December ~~12.~~2021) as an example. But before further discussion of the ERA5 results, we conducted a similar analysis of ENSO contribution using the CERES data (for the period January 2002–December 2021) and compared the results of the two datasets (Fig. S3). The remarkably consistent patterns between ERA5- and CERES-based ENSO contributions suggest that the ERA5 data is able to reproduce the essential features of ENSO-caused variations in CREs.

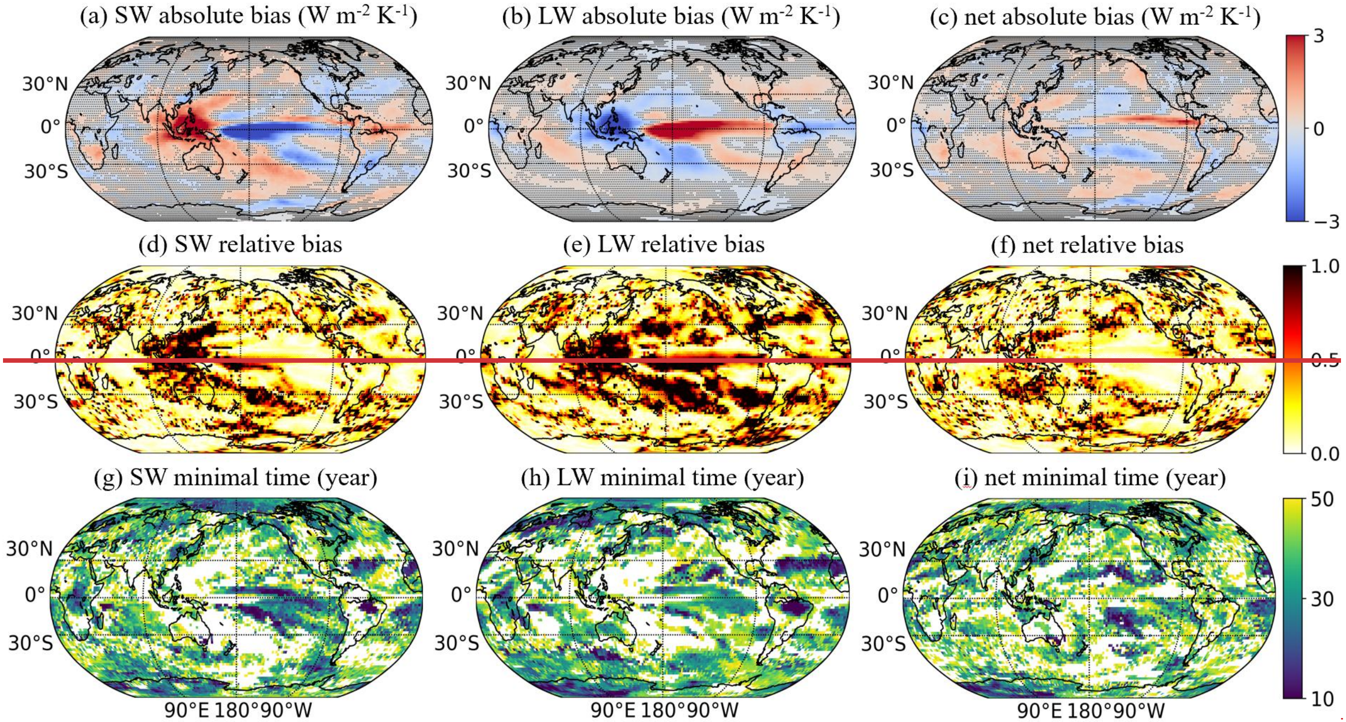
(a) SW absolute bias (W m-2 K-1)
(b) LW absolute bias (W m-2 K-1)
(c) net absolute bias (W m-2 K-1)
(d) SW relative bias
(e) LW relative bias
(f) net relative bias
(g) SW minimal time (year)
(h) LW minimal time (year)
(i) net minimal time (year)
30°N
0°
30°S
90°E 180° 90°W
3
0
−3
1.0
0.5
0.0
50
30
10

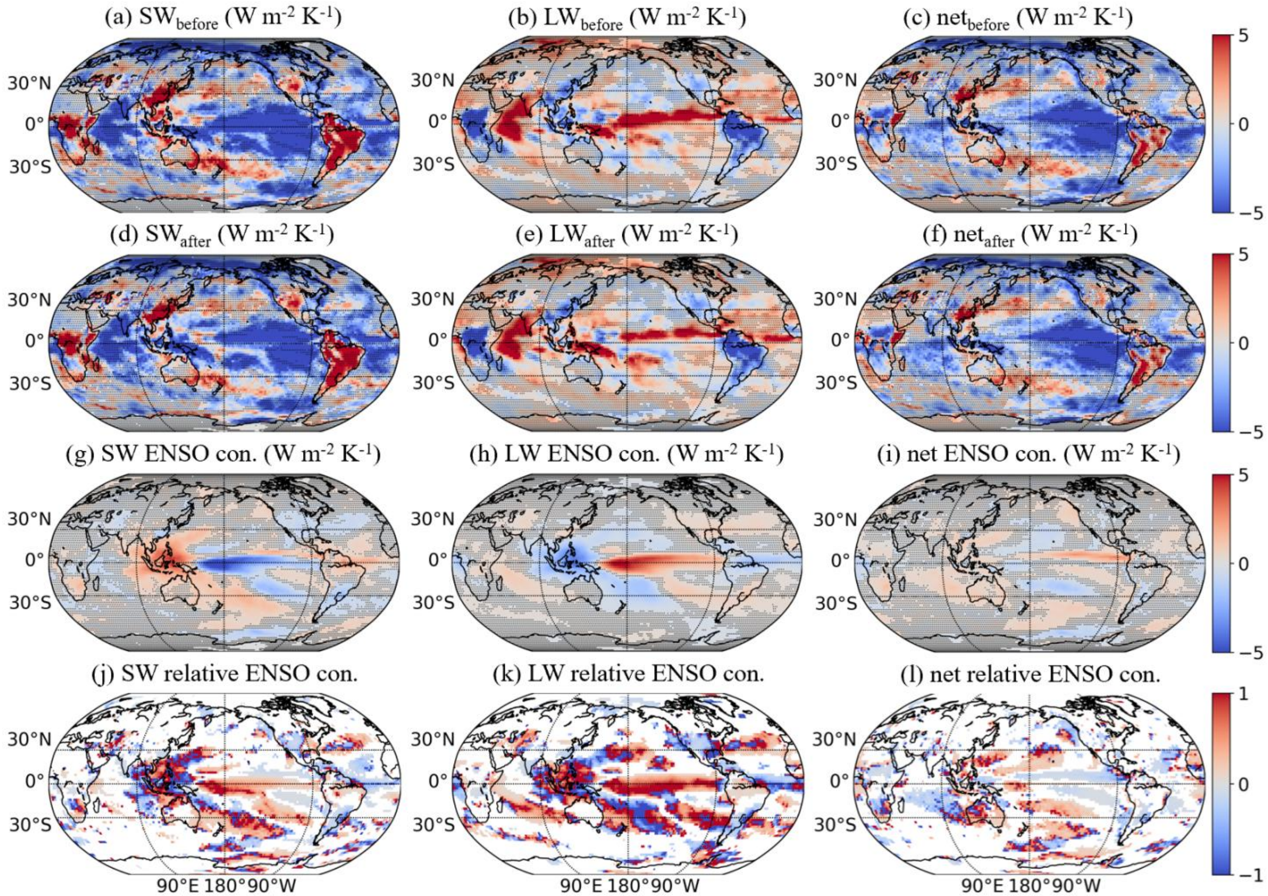

Figure 4: A sample analysis~~Spatial distributions and timescales~~ of~~ the~~ ENSO contribution to~~related bias in~~ cloud feedback estimates for CRE_{SW} (left column), CRE_{LW} (middle column), and CRE_{net} (right column), derived from ERA5 data during January ~~different cloud radiative effects, taking the period of 01.~~1982–December ~~12.~~2021~~ as an example~~. (a–c) Cloud feedback estimates before ENSO correction~~Maps of the absolute ENSO-related bias in (a) CRE_{SW}, (b) CRE_{LW}, and (c) CRE_{net}~~. (d–f) Cloud feedback estimates after ENSO correction. (g–i) ENSO contribution (a–c minus d–f). (j–l) Relative ENSO contribution (g–i divided by a–c). In panels (a–i), black dots denote grids with statistically insignificant partial regression coefficient of ONI (i.e., b in Eq. 1) for either GMST or respective CRE at the 95% confidence level. In panels (j–l), these insignificant grids are masked in white.~~Maps of the relative ENSO-related bias (the absolute bias divided by the cloud feedback estimates) in (d) CRE_{SW}, (e) CRE_{LW}, and (f) CRE_{net}. (g–i) Maps of the "ENSO effect minimal time" for (g) CRE_{SW}, (h) CRE_{LW}, and (i) CRE_{net}.~~

The ENSO contribution~~absolute bias~~ shown in Fig. ~~4a~~4g–~~c~~i can be explained by the combined effects of ONI-explained variations in GMST (4%) and CREs~~cloud radiative effects~~, as discussed in Figs. 2–3. Again, as expected~~Furthermore~~, the resulting patterns align closely with previous studies that documented ~~revealing~~ ENSO's influence on cloud properties (Yang et al., 2016; Li et al., 2021; Liu et al., 2023) and the associated physical mechanisms (Taschetto et al., 2020). During the warm phase of ENSO (e.g., El Niño events), the anomalous warming of surface waters in the central to eastern tropical Pacific weakens the Walker circulation, suppressing updrafts over the western Pacific while enhancing convection over the central to eastern Pacific. These dynamic changes affect cloud formation and development, resulting in more and deeper~~a larger~~ (less and shallower~~smaller~~) clouds ~~fraction with colder (warmer) cloud top temperatures~~ over regions such as the central (western) tropical Pacific. Consequently, ENSO-driven changes in cloud properties lead to a negative (positive) contribution to~~bias in~~ shortwave cloud feedback estimates over the corresponding regions (Fig. ~~4a~~4g) and an almost opposite one for longwave (Fig. ~~4b~~4h), together leading to relatively weak and less distinct influence ~~bias~~ in the net cloud feedback estimates (Fig. ~~4c~~4i). Such physical consistency further validates the reliability of our regression-based ~~de~~ENSO-correction method.

Figure 4~~dj–f~~l shows the distributions of the relative ENSO~~-related~~ contribution, which is calculated as the ratio between ENSO contribution (Fig. 4g–i) and the original cloud feedback estimates (Fig. 4a–c)~~bias~~. ~~As expected, t~~The ratio reaches ±1 (dark reddish and bluish ~~blackish~~ shades) over a substantial part of low- to mid-latitude oceans, indicating comparable ENSO- and non-ENSO-forced cloud feedback over these regions. But, by definition, the robustness of this relative metric suffers from near zero denominators and should be taken with caution.

As shown ~~mentioned~~ in Fig. 2, the impact of ENSO on GMST varies depending on the period under examination. To quantify this timescale dependence~~it~~, we calculate the ~~relative~~ ENSO contribution~~-related bias~~ (e.g., Fig. ~~4d~~4g–~~f~~i) for the same range of possible periods by applying each time window across the entire 72 years and use a metric we call~~introduce the concept of~~ "ENSO effect minimal time". This metric is defined as the shortest time window beyond~~(and all longer time windows), for~~ which~~,~~ the mean magnitude of ENSO contribution~~the relative bias~~ (ignoring the sign) falls and remains below 1 W m^{-2} K^{-1} (i.e., $|\overline{ENSO\ con.}| < 1\ W\ m^{-2}\ K^{-1}$), or beyond which the partial regression coefficient of ONI (i.e., b in Eq. 1) for either GMST or CRE becomes and remains statistically insignificant at the 95% confidence level. The threshold of 1 W m^{-2} K^{-1} is chosen to demonstrate a non-negligible ENSO contribution relative to the local cloud feedback estimates, which is typically on the order of several W m^{-2} K^{-1}, as simulated by current GCMs (Forster et al., 2021; Ceppi & Nowack, 2021; 301 Zelinka et al., 2016; Myers et al., 2021)~~is smaller than 0.5 (i.e.,~~ $\cancel{|\overline{relative\ bias}| < 0.5}$~~). This definition indicates that for periods longer than the "ENSO effect minimal time", the ENSO-related bias in cloud feedback is expected to be smaller than the non-ENSO part~~.

Figure ~~4g–i~~5 presents the spatial distribution of "ENSO effect minimal time" ~~maps~~ for CRE_{SW}, CRE_{LW}, and CRE_{net}, revealing complex patterns and notable differences among the three variables. In most subtropical regions, the minimal time is shorter than ~~the maximal time window in this study (5~~30 years (bluish to greenish shades). However, in some tropical and mid-latitude regions, particularly over the Pacific Ocean, the mean ENSO contribution~~relative bias is~~ never consistently falls below 1 W m^{-2} K^{-1} or becomes statistically insignificant ~~0.5~~ within time windows up to 50 years (~~marked by~~ white shades).

These results align with the slow decay of ENSO impact on GMST (Fig. 2c) and the patterns revealed for ENSO impact on CREs (Fig. 3d–f), illustrating~~e~~ clearly that ENSO contributes ~~drives a~~ significantly ~~bias in~~to the assessment of long-term cloud feedback to global warming, especially over the Pacific and~~or~~ during relatively short periods characterized by intense ENSO activity.

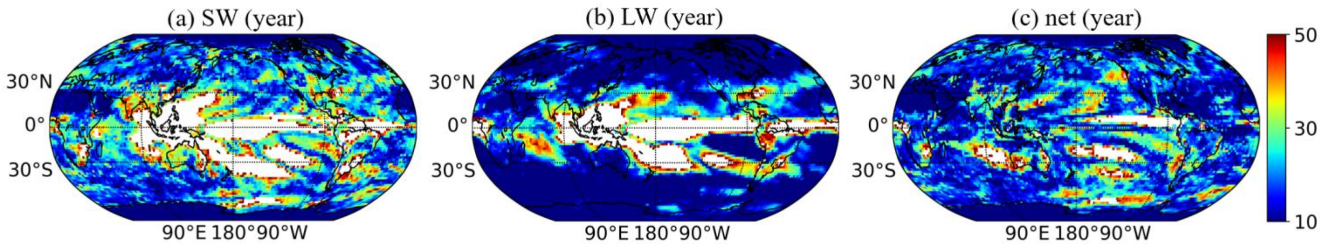

Figure 5: Maps of "ENSO effect minimal time" for different CREs, derived from ERA5 data during January 1982–December 2021. (a) CRE$_{SW}$, (b) CRE$_{LW}$, and (c) CRE$_{net}$. Regions masked in white denote grids where ENSO contribution never consistently falls below 1 W m^{-2} K^{-1} or becomes statistically insignificant within time windows up to 50 years.

Figure 6 then gives the ENSO contribution to global-mean CREs as a function of the time window. The corresponding results derived from CERES measurements, ERA5 data during the CERES period, and ERA5 data during the representative 40-year subset are also shown. As expected, the results change with time and converge toward small values (about 0.1, 0.0, and 0.1 W m^{-2} K^{-1} for CRE$_{SW}$, CRE$_{LW}$, and CRE$_{net}$, respectively) due to the cancellation of positive and negative local ENSO contributions across different regions. This convergence also agrees well with the revealed behaviour of ENSO impact on GMST in Fig. 2c.

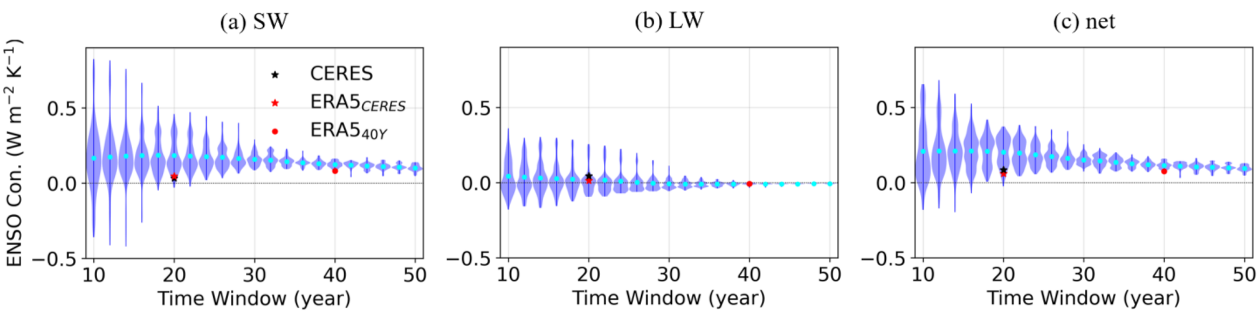

Figure 6: Violin plots of ENSO contribution to global-mean CREs, derived from ERA5 data during January 1950–December 2021. (a) CRE$_{SW}$, (b) CRE$_{LW}$, and (c) CRE$_{net}$. The black star, red star, and red dot denote the results from CERES measurements, ERA5 data during the CERES period, and ERA5 data during the exampled 40-year period, respectively.

To provide a ~~partly~~ partial validation of~~e~~ our findings within current climate models, taking the CRE$_{net}$ as an example, we analyzed the "ENSO effect minimal time" and the global-mean ENSO contribution for ~~12~~ 11 GCM simulations of the historical experiments (Figs. S4–~~S-~~5). Though obvious inter-model discrepancies exist, the general message ~~of these results is~~ that ~~the~~ ENSO can significantly ~~bias~~ affect long-term cloud feedback estimates remains consistent. The discrepancies between the models indicate deficiencies in the ability of models to accurately represent ~~the~~ ENSO, global warming, and their relative impacts on GMST and clouds properties (Bellenger et al., 2014; Coburn and Pryor, 2021).

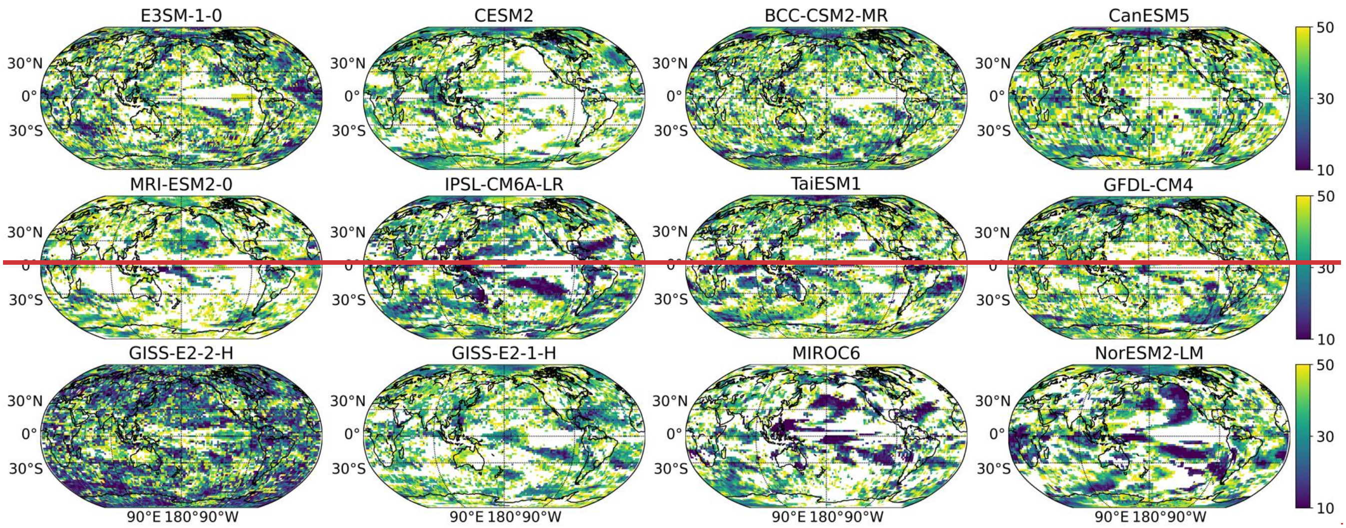

~~**Figure 5: Maps of the "ENSO effect minimal time" for CRE_{net} from the CMIP6 historical experiment during 01.1950–12.2014. The name of the corresponding model is titled.**~~

3.4 ENSO contribution to ~~related bias in estimating~~ cloud feedback projections~~with the abrupt-4×CO_2 experiment~~

To link our findings to climate projections, we analyze the first 150 years of 11 GCM simulations from the abrupt-4×CO_2 ~~GCM~~ experiment~~ data, using the first 150 years of simulations~~. Figures ~~6 and~~ 7 gives the spatial distribution of ENSO contribution to CRE_{net}, the corresponding relative contribution is shown in Fig. 8~~absolute and relative bias in CRE_{net}, respectively~~.

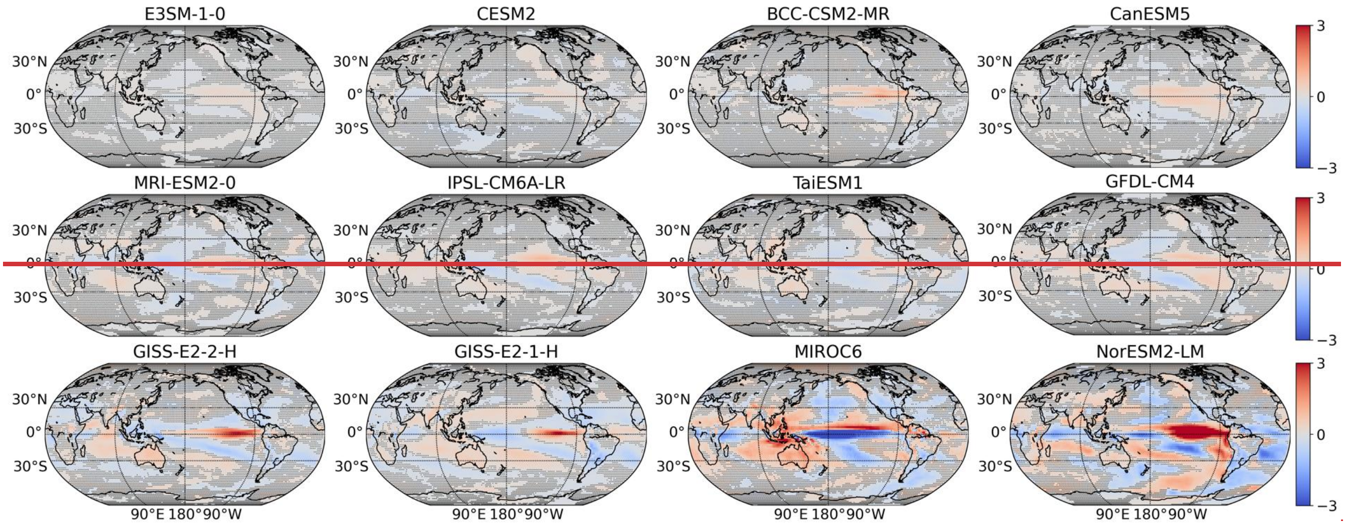

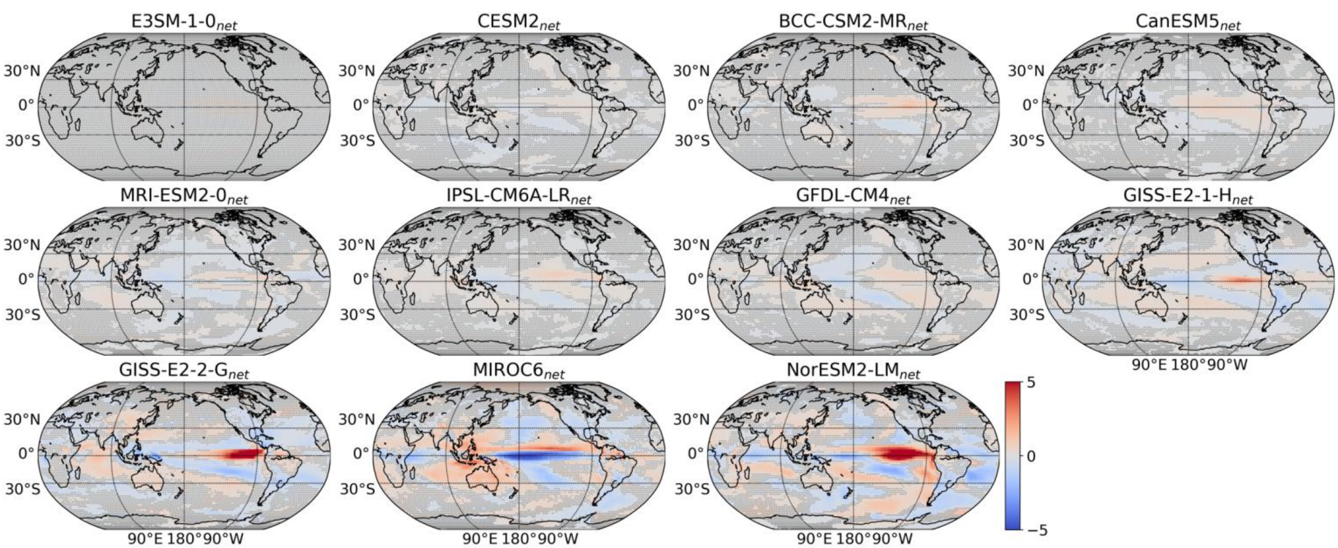

Figure ~~6~~7: Maps of the ~~absolute~~ ENSO contribution to~~-related bias in~~ CRE$_{net}$, derived from GCM simulations from the abrupt-4×CO_2 experiment during the first 150 years. The name of the corresponding model is indicated in each panel. Black dots denote grids with statistically insignificant partial regression coefficient of ONI (i.e., b in Eq. 1) for either GMST or CRE at the 95% confidence level~~titled~~.

Again, ~~on one hand,~~ significant ENSO contributions~~-related biases~~ are captured worldwide, especially over the Pacific Ocean. However, substantial~~; on the other hand, obvious~~ discrepancies in terms of both patterns and magnitudes exist among GCMs. More specifically, Fig. ~~6~~ 7 suggests a~~n~~ predominantly ~~overall~~ positive ENSO contribution ~~bias~~ (reddish shades) over the eastern tropical Pacific and a~~n~~ predominantly ~~overall~~ negative ENSO contribution ~~bias~~ (bluish shades) over the western tropical Pacific, indicating that the analyzed GCMs capture~~d~~ the broad structure~~typical pattern~~ of cloud response to ENSO to a certain degree. But the specific ~~corresponding~~ magnitudes and detailed spatial features vary considerably across~~dramatically between~~ the ~~12~~ 11 models. For instance, simulations from GISS-E2-2-G,~~, GCMs like~~ MIROC6 and NorESM2-LM ~~even~~ show that ~~the absolute~~ ENSO contribution to ~~related bias in~~ cloud feedback estimates remains on the order of ~~over 150 years reaches~~ a few W m^{-2} K^{-1} over extensive regions, even for a 150-year period ~~a large portion of the world~~, which is comparable to the local cloud feedback ~~estimations~~ estimates (Forster et al., 2021; Ceppi & Nowack, 2021; Zelinka et al., 2016; Myers et al., 2021). These findings also align with and extend previous studies that identified robust correlations between interannual and long-term cloud feedback (e.g., Zhou et al., 2015; Dessler and Forster, 2018; Davis et al., 2024) by highlighting the potential modulating role of ENSO contributions.

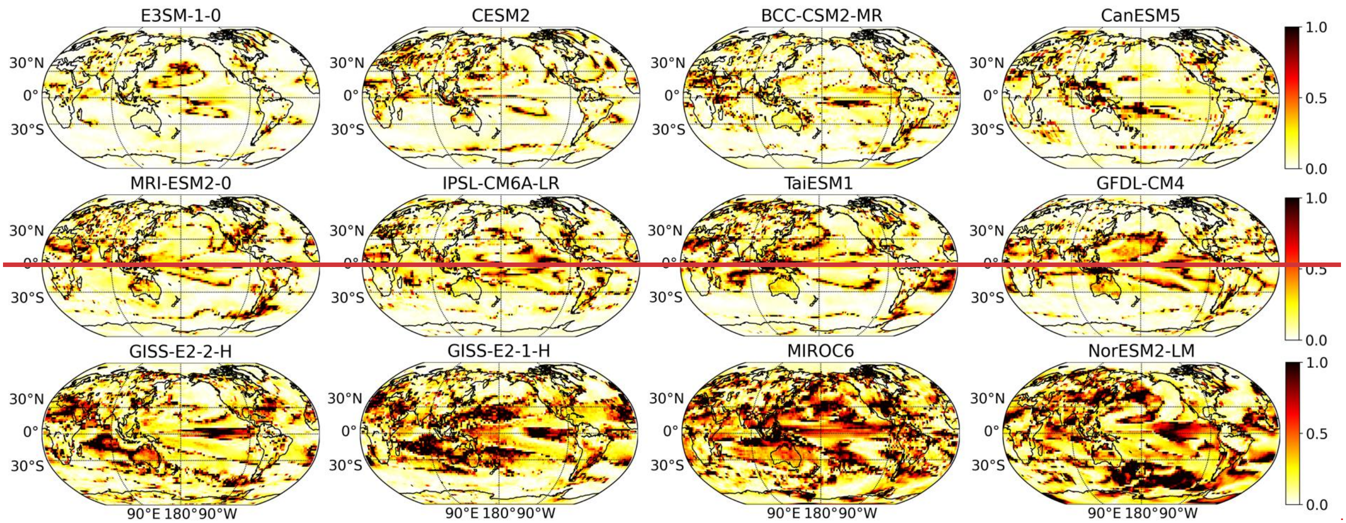

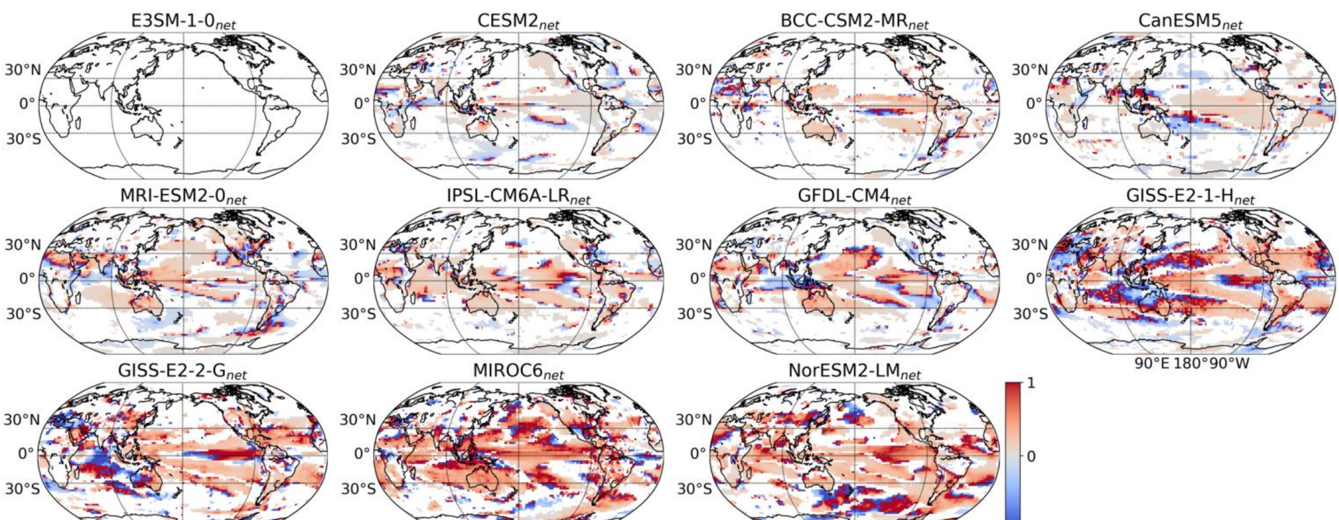

Figure ~~7~~8: Maps of the relative ENSO contribution to ~~related bias in~~ CRE$_{net}$, derived from GCM simulations from the abrupt-4×CO_2 experiment during the first 150 years. The name of the corresponding model is indicated in each panel. Grids with statistically insignificant partial regression coefficient of ONI (i.e., b in Eq. 1) for either GMST or CRE at the 95% confidence level are masked in white ~~titled~~.

ENSO contribution to global-mean CRE_{net} (Fig. 9) shows large inter-model spread as well~~Compared to the absolute bias, the relative bias (Fig. 7) shows even more significant model uncertainties regarding both the pattern and the magnitude~~. As discussed above~~before~~, these differences indicate deficiencies of models in accurately representing ~~the~~ ENSO, global warming, and their relative impacts on GMST and clouds (Bellenger et al., 2014; Coburn and Pryor, 2021). For example, previous studies suggest that, compared to observations, ~~current~~ many GCMs present a too-strong equatorial Pacific cold tongue (Jiang et al., 2021) and fail to capture the recent strengthening of the west-to-east equatorial Pacific SST gradient (Seager et al., 2019). These two deficiencies introduce critical uncertainties into ~~the~~ projections of ENSO, and hence clouds, under global warming (e.g., Guilyardi et al., 2020; Beobide-Arsuaga et al., 2021). The timeseries of GMST and global-mean CREnet for two representative GCMs (E3SM-1-0 and NorESM2-LM) are also shown in Fig. S6. The results suggest a clear separation between the trend- and ONI-related variations achieved by our regression-based ENSO-correction method, thereby providing further validation for the ENSO contribution obtained by this method.

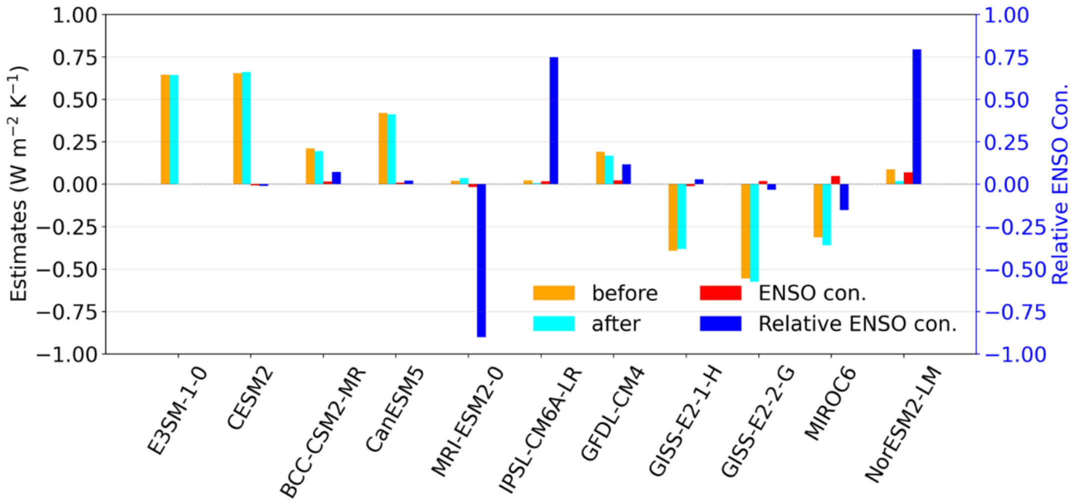

Figure 9: Bar charts of ENSO contribution to global-mean CRE_{net}, derived from GCM simulations from the abrupt-4×CO_2 experiment during the first 150 years. The orange and cyan bars indicate global-mean cloud feedback estimates before and after ENSO correction, respectively. The red and blue bars indicate ENSO contribution (orange minus cyan bars) and relative ENSO contribution (red divided by orange bars; right y-axis), respectively.

4 Discussion

ENSO is a natural interannual climate phenomenon associated with anomalous sea-~~-~~surface temperature and pressure in the tropical Pacific Ocean. It has been shown to impact global temperature and cloud properties (Davey et al., 2014; Cai et al., 2019; Taschetto et al., 2020), and consequently, it affects the accuracy of cloud feedback estimates under global warming (Zhou et al., 2015; Uribe et al., 2022; Richardson et al., 2022; Jin et al., 2024). This study quantifies such ENSO contribution using~~es~~ 72 years of ERA5 data and 150 years of~~long-term~~ simulations conducted by ~~12~~ 11 GCMs~~ to quantify such ENSO~~

~~related biases~~. The results reveal that regression-based cloud feedback ~~estimations~~ estimates are susceptible to a significant ENSO~~-related bias~~ impact, even ~~over~~ on decadal and centennial timescales~~decades~~. A regression-based ~~de~~ENSO-correction method~~ procedure~~ was then applied to correct for ENSO's influence and quantify its contribution~~quantify the bias~~. The findings show that the magnitude of th~~e bias~~is contribution exhibits strong regional and temporal dependence~~varies across different regions and timescales~~. In most subtropical regions, ~~ENSO-related bias is smaller than~~ the contribution remains statistically significant and~~non-ENSO part only over timescale of decades. However, in many tropical regions, the bias~~ can exceed 1 W m^{-2} K^{-1}~~the non-ENSO part~~, even for periods longer than 50 years (the maximal time window analyzed). These results highlight the importance of incorporating an ~~de~~ENSO-correction procedure when assessing the forced cloud feedback~~estimating climate trends~~, particularly in tropical regions and for short periods characterized by~~over the Pacific Ocean or during periods of~~ intense ENSO activity.

The study acknowledges several limitations, including its inability to account for non-linear or delayed ENSO effects (Compo and Sardeshmukh, 2010) and the sensitivity of the ~~'ENSO~~ "ENSO effect minimal time"~~'~~ to the chosen threshold and used dataset~~models~~. As a result, the findings should be considered conservative estimates and the quantitative conclusions should be interpreted with caution, particularly in the context of GCM simulations. Notwithstanding ~~Despite~~ these limitations, the study provides a straightforward method to approximate ENSO contribution~~-related biases~~, offering valuable insights into the influence of ENSO on cloud feedback estimates. The implications of this research are twofold~~significant~~. First, it quantitatively assesses~~quantifies~~ the spatial distribution and timescales of ~~the~~ ENSO contribution to regression-based~~-related bias in~~ cloud feedback estimates. Second, given the known deficiencies in GCMs' representation of ENSO and its dynamics (Bellenger et al., 2014; Coburn and Pryor, 2021; Jiang et al., 2021; Seager et al., 2019), coupled with substantial~~as well as~~ uncertainties in future ENSO projections (Guilyardi et al., 2020; Beobide-Arsuaga et al., 2021), the revealed significant impact of ENSO on warming and cloud properties highlights a critical challenge~~s~~ to the reliability of climate projections.

References

Angell, J. K.: Tropospheric temperature variations adjusted for El Niño, 1958–1998, J. Geophys. Res. Atmos., 105, 11841–11849, doi:10.1029/2000JD900044, 2000.

Bellenger, H., Guilyardi, E., Leloup, J., Lengaigne, M. and Vialard, J.: ENSO representation in climate models: From CMIP3 to CMIP5, Clim. Dyn., 42, 1999–2018, doi:10.1007/s00382-013-1783-z, 2014.

Beobide-Arsuaga, G., Bayr, T., Reintges, A. and Latif, M.: Uncertainty of ENSO-amplitude projections in CMIP5 and CMIP6 models, Clim. Dyn., 56, 3875–3888, doi:10.1007/s00382-021-05673-4, 2021.

Binder, H., Boettcher, M., Joos, H., Sprenger, M. and Wernli, H.: Vertical cloud structure of warm conveyor belts–a comparison and evaluation of ERA5 reanalysis, CloudSat and CALIPSO data, Weather Clim. Dyn., 1, 577–595, doi:10.5194/wcd-1-577-2020, 2020.

Cai, W. et al.: Pantropical climate interactions, Science, 363, eaav4236, doi:10.1126/science.aav423, 2019.

Ceppi, P. and Nowack, P.: Observational evidence that cloud feedback amplifies global warming, Proc. Natl. Acad. Sci., 118, e2026290118, doi:10.1073/pnas.2026290118, 2021.

Chen, T., Rossow, W.B., and Zhang, Y.: Radiative effects of cloud-type variations, J. Clim., 13, 264–286, doi:10.1175/1520-0442(2000)013<0264:REOCTV>2.0.CO;2, 2000.

Clement, A. C., Burgman, R. and Norris, J. R.: Observational and Model Evidence for Positive Low-Level Cloud Feedback, Science, 325, 460–464, doi:10.1126/science.11712, 2009.

Coburn, J. and Pryor, S. C.: Differential Credibility of Climate Modes in CMIP6, J. Clim., 34, 8145–8164, doi:10.1175/JCLI-D-21-0359.1, 2021.

Compo, G. P. and Sardeshmukh, P. D.: Removing ENSO-related variations from the climate record, J. Clim., 23, 1957–1978, doi:10.1175/2009JCLI2735.1, 2010.

Davey, M., Brookshaw, A. and Ineson, S.: The probability of the impact of ENSO on precipitation and near-surface temperature, Clim. Risk Manag., 1, 5–24, doi:10.1016/j.crm.2013.12.002, 2014.

Davis, L. L. B., Thompson, D. W. J., Rugenstein, M. and Birner, T.: Links between internal variability and forced climate feedbacks: The importance of patterns of temperature variability and change. Geophys. Res. Lett., 51, e2024GL112774, doi.org/10.1029/2024GL112774, 2024.

Dessler, A. E.: A determination of the cloud feedback from climate variations over the past decade, Science, 330, 1523–1527, doi:10.1126/science.1192546, 2010.

Dessler, A. E. and Forster, P. M.: An estimate of equilibrium climate sensitivity from interannual variability. J. Geophys. Res. Atmos., 123, 8634-8645, https://doi.org/10.1029/2018JD028481, 2018.

Eleftheratos, K., Zerefos, C., Varotsos, C. and Kapsomenakis, I.: Interannual variability of cirrus clouds in the tropics in el niño southern oscillation (ENSO) regions based on international satellite cloud climatology project (ISCCP) satellite data, Int. J. Remote Sens., 32, 6395–6405, doi:10.1080/01431161.2010.510491, 2011.

Eyring, V., Bony, S., Meehl, G. A., Senior, C. A., Stevens, B., Stouffer, R. J., and Taylor, K. E.: Overview of the Coupled Model Intercomparison Project Phase 6 (CMIP6) experimental design and organization, Geosci. Model Dev., 9, 1937–1958, doi:10.5194/gmd-9-1937-2016, 2016.

Eyring, V., Gillett, N. P., Achuta Rao, K. M., Barimalala, R., Barreiro Parrillo, M., Bellouin, N. et al.: Human Influence on the Climate System, in Climate Change 2021: The Physical Science Basis, Contribution of Working Group I to the Sixth Assessment Report of the Intergovernmental Panel on Climate Change (Cambridge University), doi:10.1017/9781009157896.005, 2021.

Forster, P., Storelvmo, T., Armour, K., Collins, W., Dufresne, J. L., Frame, D. et al.: The Earth's Energy Budget, Climate Feedbacks, and Climate Sensitivity, in Climate Change 2021: The Physical Science Basis, Contribution of Working Group I to the Sixth Assessment Report of the Intergovernmental Panel on Climate Change (Cambridge University), doi:10.1017/9781009157896.009, 2021.

Glantz, M. H. and Ramirez, I. J.: Reviewing the oceanic Nino index (ONI) to enhance societal readiness for El Niño's impacts, Int. J. Disaster Risk Sci., 11, 394–403, doi:10.1007/s13753-020-00275-w, 2020.

Guan, B. and Nigam, S.: Pacific Sea Surface Temperatures in the Twentieth Century: An Evolution-Centric Analysis of Variability and Trend, J. Clim., 21, 2790–2809, doi:10.1175/2007JCLI2076.1, 2008.

Guilyardi, E., Capotondi, A., Lengaigne, M., Thual, S. and Wittenberg, A. T.: ENSO Modeling: History, Progress, and Challenges, in El Niño Southern Oscillation in a Changing Climate (American Geophysical Union), doi:10.1002/9781119548164.ch9, 2020.

Gulev, S. K., Thorne, P. W., Ahn, J., Dentener, F. J., Domingues, C. M., Gong, D. et al.: Changing State of the Climate System, in Climate Change 2021: The Physical Science Basis, Contribution of Working Group I to the Sixth Assessment Report of the Intergovernmental Panel on Climate Change (Cambridge University), doi:10.1017/9781009157896.004, 2021.

Hamed, K. H. and Rao, A. R.: A modified Mann-Kendall trend test for autocorrelated data, J. Hydrol., 204, 182-196, doi:10.1016/S0022-1694(97)00125-X, 1998.

Hersbach, H., Bell, B., Berrisford, P., Hirahara, S., Horányi, A., Muñoz-Sabater, J. et al.: The ERA5 global reanalysis, Q. J. R. Meteorol. Soc., 146, 1999–2049, doi:10.1002/qj.3803, 2020.

Hersbach, H. Bell, B., Berrisford, P., Biavati, G., Horányi, A., Muñoz-Sabater, J. et al.: ERA5 monthly averaged data on single levels from 1940 to present [Dataset], Copernicus Climate Change Service (C3S) Climate Data Store (CDS), doi:10.24381/cds.f17050d7, 2023.

Hope, P., Henley, B. J., Gergis, J., Brown, J. and Ye, H.: Time-varying spectral characteristics of ENSO over the Last Millennium, Clim. Dyn., 49, 1705–1727, doi:10.1007/s00382-016-3393-z, 2017.

Hussain, M. M. and Mahmud, I.: pyMannKendall: a python package for non parametric Mann Kendall family of trend tests [Software], J. Open Source Softw., 4, 1556, doi:10.21105/joss.01556, 2019.

Jiang, W., Huang, P., Huang, G. and Ying, J.: Origins of the Excessive Westward Extension of ENSO SST Simulated in CMIP5 and CMIP6 Models, J. Clim., 34, 2839–2851, doi:10.1175/JCLI-D-20-0551.1, 2021.

Jin, D., Kramer R. J., Oreopoulos, L. and Lee D.: ENSO disrupts boreal winter CRE feedback, J. Clim., 37, 585–603, doi:10.1175/JCLI-D-23-0282.1, 2024.

Johnson, N. C.: How many ENSO flavors can we distinguish?, J. Clim., 26, 4816–4827, doi:10.1175/JCLI-D-12-00649.1, 2013.

Kelly, P. M. and Jones, P. D.: Removal of the El Niño-Southern Oscillation signal from the gridded surface air temperature data set, J. Geophys. Res. Atmos., 101, 19013–19022, doi:10.1029/96JD01173, 1996.

Li, Y. et al.: Pairwise-rotated EOFs of global cloud cover and their linkages to sea surface temperature, Int. J. Climatol., 41, 2342–2359, doi:10.1002/joc.6962, 2021.

Liu, H., Koren, I., Altaratz, O. and Chekroun, M. D.: Opposing trends of cloud coverage over land and ocean under global warming, Atmos. Chem. Phys., 23, 6559–6569, doi:10.5194/acp-23-6559-2023, 2023.

Loeb, N. G., Doelling, D. R., Wang, H., Su, W., Nguyen, C., Corbett, J. G., et al.: Clouds and the earth's radiant energy system (CERES) energy balanced and filled (EBAF) top-ofatmosphere (TOA) edition-4.0 data product, J. Clim., 31, 895-918, doi.org/10.1175/JCLI-D-17-0208.1, 2018.

Madenach, N., Carbajal Henken, C., Preusker, R., Sourdeval, O. and Fischer, J.: Analysis and quantification of ENSO-linked changes in the tropical atlantic cloud vertical distribution using 14 years of MODIS observations, Atmos. Chem. Phys., 19, 13535–13546, doi:10.5194/acp-19-13535-2019, 2019.

Myers, T. A., Scott, R. C., Zelinka, M. D., Klein, S. A., Norris, J. R. and Caldwell, P. M.: Observational constraints on low cloud feedback reduce uncertainty of climate sensitivity, Nat. Clim. Chang., 11, 501–507, doi:10.1038/s41558-021-01039-0, 2021.

Neelin, J. D., Battisti, D. S., Hirst, A. C., Jin, F. F., Wakata, Y., Yamagata, T. et al.: ENSO theory, J. Geophys. Res.: Oceans, 103, 14261–14290, doi:10.1029/97JC03424, 1998.

Park, S. and Leovy C. B.: Marine low-cloud anomalies associated with ENSO, J. Clim., 17, 3448–3469, doi:10.1175/1520-0442(2004)017<3448:MLAAWE>2.0.CO;2, 2004.

Penland, C. and Matrosova, L.: Studies of El Niño and interdecadal variability in tropical sea surface temperatures using a nonnormal filter, J. Clim., 19, 5796–5815, doi:10.1175/JCLI3951.1, 2006.

Richardson, M. T., Roy, R. J. and Lebsock, M. D.: Satellites suggest rising tropical high cloud altitude: 2002–2021, Geophys. Res. Lett., 49, e2022GL098160, doi:10.1029/2022GL098160, 2022.

Seager, R., Cane, M., Henderson, N., Lee, D. E., Abernathey, R. and Zhang, H.: Strengthening tropical Pacific zonal sea surface temperature gradient consistent with rising greenhouse gases, Nat. Clim. Chang., 9, 517-522, doi:10.1038/s41558-019-0505-x, 2019.

Stephens, G. L., Li, J., Wild, M., Clayson C. A., Loeb, N., Kato, S. et al.: An update on Earth's energy balance in light of the latest global observations, Nat. Geosci., 5, 691–696, doi:10.1038/ngeo1580, 2012.

Stubenrauch, C. J., Rossow, W. B., Kinne S., Ackerman, S., Cesana G., Chepfer, H. et al.: Assessment of global cloud datasets from satellites: Project and database initiated by the GEWEX radiation panel, Bull. Amer. Meteor. Soc., 94, 1031–1049, doi:10.1175/BAMS-D-12-00117.1, 2013.

Taschetto, A. S., Ummenhofer, C. C., Stuecker, M. F., Dommenget, D., Ashok, K., Rodrigues, R. R. et al.: ENSO Atmospheric Teleconnections, in El Niño Southern Oscillation in a Changing Climate (American Geophysical Union), doi:10.1002/9781119548164.ch14, 2020.

Teng, H. F., Lee, C. S. and Hsu, H. H.: Influence of ENSO on formation of tropical cloud clusters and their development into tropical cyclones in the western north pacific, Geophys. Res. Lett., 41, 9120–9126, doi:10.1002/2014GL061823, 2014.

Uribe, A., Bender, F. A. M. and Mauritsen, T.: Observed and CMIP6 modeled internal variability feedbacks and their relation to forced climate feedbacks, Geophys. Res. Lett., 49, e2022GL100075, doi:10.1029/2022GL100075, 2022.

Virtanen, P., Gommers, R., Oliphant, T. E., Haberland M., Reddy, T., Cournapeau, D. et al.: SciPy 1.0: Fundamental Algorithms for Scientific Computing in Python, Nat. Methods, 17, 261-272, doi:10.1038/s41592-019-0686-2., 2020.

Webb, M. J., Andrews, T., Bodas-Salcedo, A., Bony, S., Bretherton, C. S., Chadwick, R. et al.: The Cloud Feedback Model Intercomparison Project (CFMIP) contribution to CMIP6, Geosci. Model Dev., 10, 359-384, doi:10.5194/gmd-10-359-2017, 2017.

Yang, Y., Russell, L. M., Xu, L., Lou, S., Lamjiri, M. A., Somerville, R. C. J. et al.: Impacts of ENSO events on cloud radiative effects in preindustrial conditions: changes in cloud fraction and their dependence on interactive aerosol emissions and concentrations, J. Geophys. Res. Atmos., 121, 6321–6335, doi:10.1002/2015JD024503, 2016.

Yao, B., Teng, S., Lai, R., Xu, X., Yin, Y., Shi, C. et al.: Can atmospheric reanalyses (CRA and ERA5) represent cloud spatiotemporal characteristics?. Atmos. Res., 244, 105091, doi:10.1016/j.atmosres.2020.105091, 2020.

Zelinka, M. D., Zhou, C. and Klein, S. A.: Insights from a refined decomposition of cloud feedbacks, Geophys. Res. Lett., 43, 9259–9269, doi:10.1002/2016GL069917, 2016.

Zelinka, M. D., Myers, T. A., McCoy, D. T., Po-Chedley, S., Caldwell, P. M., Ceppi, P. et al.: Causes of higher climate sensitivity in cmip6 models, Geophys. Res. Lett., 47, 2019–085782, doi:10.1029/2019GL085782, 2020.

Zhou, C., Zelinka, M. K., Dessler, A. E., and Klein S. A.: The relationship between interannual and long-term cloud feedbacks, Geophys. Res. Lett., 42, 10–463, doi:10.1002/2015GL066698, 2015.